1
Nanoparticles Based on π-Conjugated Polymers and Oligomers for Optoelectronic, Imaging, and Sensing Applications: The Illustrative Example of Fluorene-Based Polymers and Oligomers

Irén Fischer and Albertus P.H.J. Schenning

1.1
Introduction

Nanoparticles based on π-conjugated polymers and oligomers have received considerable attention for optoelectronic and biological applications due to their small size, simple preparation method, and their tunable and exceptional fluorescent properties [1–7]. Nanoparticles are appealing for optoelectronic devices such as organic light-emitting diodes (OLEDs) [8,9], organic photovoltaic devices (OPVs) [10], and organic field-effect transistors (OFETs) [11] to gain control over the morphology of the active layer that plays a crucial role in the device performance. For example, in OPVs exciton dissociation occurs only at the interface of the donor and acceptor materials. Therefore, it is critical to control the donor–acceptor interface in order to optimize charge separation and charge migration to the electrodes [12,13]. The most common way to increase the interfacial area is by blending donor and acceptor materials making bulk heterojunction solar cells [14]. This necessary control over nanomorphology can be achieved by using nanoparticles to generate the active layer of the device [15]. Furthermore, the development of stable and fluorescent nanoparticles is interesting when combined with printing techniques to achieve large-area patterned active layers [6].

Nanoparticles based on π-conjugated systems show excellent fluorescence brightness, high absorption cross sections, and high effective chromophore density, which makes them attractive for imaging and sensing applications [1–5]. Fluorescence-based methods for probing biomolecular interactions at level of single molecules have resulted in significant advances in understanding various biochemical processes [16]. But there is currently a lack of dyes that are sufficiently bright and photostable to overcome the background fluorescence and scattering within the cell [17,18]. In addition, the photostability of the chromophore is critical for single-molecule imaging and tracking [19].

Here, an overview of the recent advances of nanoparticles based on fluorene oligomers and polymers is presented. We have chosen the illustrative example of fluorene-based π-conjugated systems to restrict this chapter but still show all aspects

Organic Electronics: Emerging Concepts and Technologies, First Edition. Edited by Fabio Cicoira and Clara Santato.

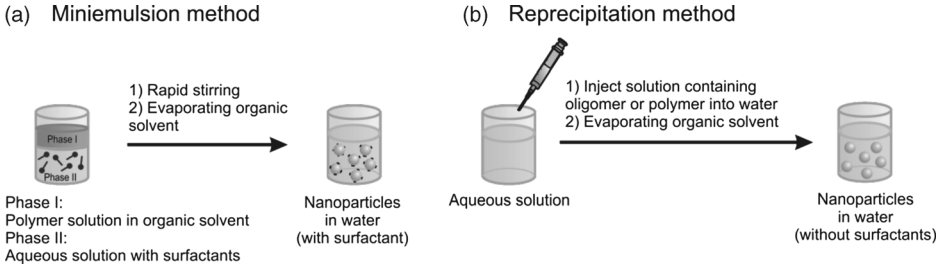

Figure 1.1 Schematic representations of the preparation of the nanoparticles (a) by using the miniemulsion method and (b) by using the reprecipitation method.

of nanoparticles based on π-conjugated polymers and oligomers. The fluorene moiety is a very favorable building block for π-conjugated systems because of its high and tunable fluorescence, high charge carrier mobility, and good solubility in organic solvents [20–24]. Furthermore, a large variety of fluorene-based polymers and oligomers can be created due to easy synthesis procedures [25,26]. Most organic nanoparticles for optoelectronic applications are prepared by the so-called miniemulsion method (Figure 1.1a) [27,28]. In this process, the π-conjugated system is dissolved in an organic solvent and then added to an aqueous solution containing surfactants. Stable nanoparticles are formed after sonication and evaporation of the organic solvent. The diameter of the nanoparticles can be reduced by increasing the surfactant concentration in the water solution or decreasing the polymer concentration in the organic solvent [29]. Nanoparticles in water for imaging and sensing applications are mostly prepared by the reprecipitation method in which a π-conjugated polymer or oligomer dissolved in THF solution is rapidly injected into water and subsequently sonicated (Figure 1.1b) [30,31].

Fluorescence energy transfer (FRET) in nanoparticles is an important tool to study their nanomorphologies for solar cells [32–34], tune their colors in OLEDs [35,36], and exploit them for sensing applications [37,38]. For an efficient energy transfer process, the emission spectrum of the donor should overlap with the absorption spectrum of the acceptor and the donor and acceptor need to be in close proximity, as the process highly depends on the distance between the donor and the acceptor (Eq. (1.1)) [39].

The Förster energy transfer rate (k_{DA}) for an individual donor–acceptor pair separated by a distance R is given by

$$k_{DA}(t) = \frac{1}{\tau_D}\left(\frac{R_0}{R}\right)^6, \tag{1.1}$$

where R_0 is the Förster radius and τ_D is the natural lifetime of the donor in the absence of acceptors.

In the first part of this chapter, nanoparticles based on fluorene polymers and their application in optoelectronic devices, biosensing, and imaging will be discussed. In the second part, nanoparticles based on fluorene oligomers will be described. Water-

soluble fluorene-based polyelectrolytes [40–43] and so-called hybrid nanoparticles [44,45] are beyond the scope of this chapter.

1.2
Nanoparticles Based on Fluorene Polymers

1.2.1
Optoelectronic Applications

1.2.1.1 Characterization of Nanoparticles

Most polyfluorene-based organic nanoparticles for optoelectronic applications are prepared by the so-called miniemulsion method [27,28]. The sizes of polyfluorene-based particles prepared by this method range typically between 50 and 500 nm [29]. Recently, small particles were prepared by *in situ* metal-catalyzed polymerization of a bifunctional diacetylene fluorene in aqueous miniemulsion yielding particles of around 30 nm [46]. This new method provides access to stable particles with sizes small enough for the preparation of ultrathin films [47], and is not limited to polymers with a high solubility in organic solvents [46]. The emission wavelength of the polyfluorene nanoparticles in comparison with the polymer in chloroform was shifted from blue to green and the quantum yield was decreased, which is normally seen for π-conjugated polymer films (Figure 1.2). Interestingly, copolymerization of a perylene diimide dye equipped with two acetylene functionalities with the fluorene moiety could also be carried out *in situ* in the aqueous solution. The emission wavelength could be varied from blue for the pure fluorene polymer to red for 2% incorporated perylene diimide dye in the copolymer due to (partial) energy transfer. The emission spectra and the quantum yields of the nanoparticles in aqueous solution were found to resemble the solution-cast film

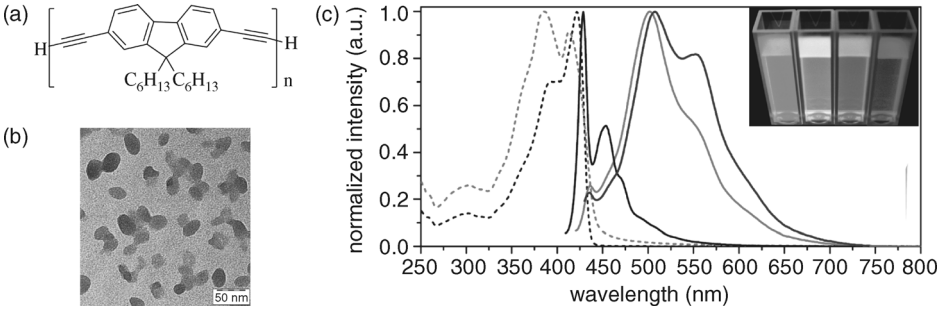

Figure 1.2 (a) Chemical structure of the fluorene–acetylene polymer. (b) Transmission electron microscopy (TEM) image of fluorene nanoparticles. (c) Absorption (dashed line) and fluorescence (solid line) spectra of aqueous dispersions (light gray), chloroform solutions (black), and thin films (dark gray) of polyfluorene nanoparticles. The inset shows the photograph of dilute polymer dispersion with 0, 0.1, 0.2, and 0.8% incorporated perylene diimide dye. (Reprinted with permission from Ref. [46]. Copyright 2009, American Chemical Society.)

samples showing that the morphology in the nanoparticles is not changed during drop casting (Figure 1.2) [46].

1.2.1.2 Nanoparticle Film Fabrication and Characterization

Nanoparticle films deposited by spin coating onto glass substrates have been studied by Landfester *et al.* [48]. Layers of polyfluorene (PF2/6 and PF11112, Figure 1.3a) nanoparticles that were formed via the miniemulsion method were prepared. For particles of polyfluorenes (PF2/6), the particle structure can be well detected with atomic force microscopy (AFM) in the deposited layers. Annealing above the glass transition temperature resulted in coalescence of the particles, and larger structures were formed [48]. Due to the low glass transition temperature of PF11112, the particles combined and formed larger domains on the substrate already at room temperature. This method allows the construction of multilayer structures composed of alternating layers formed from an organic solvent and layers formed by deposition of aqueous polymer nanoparticles. In such a way, multilayers can be prepared from polymers that are soluble in the same solvent [48,49].

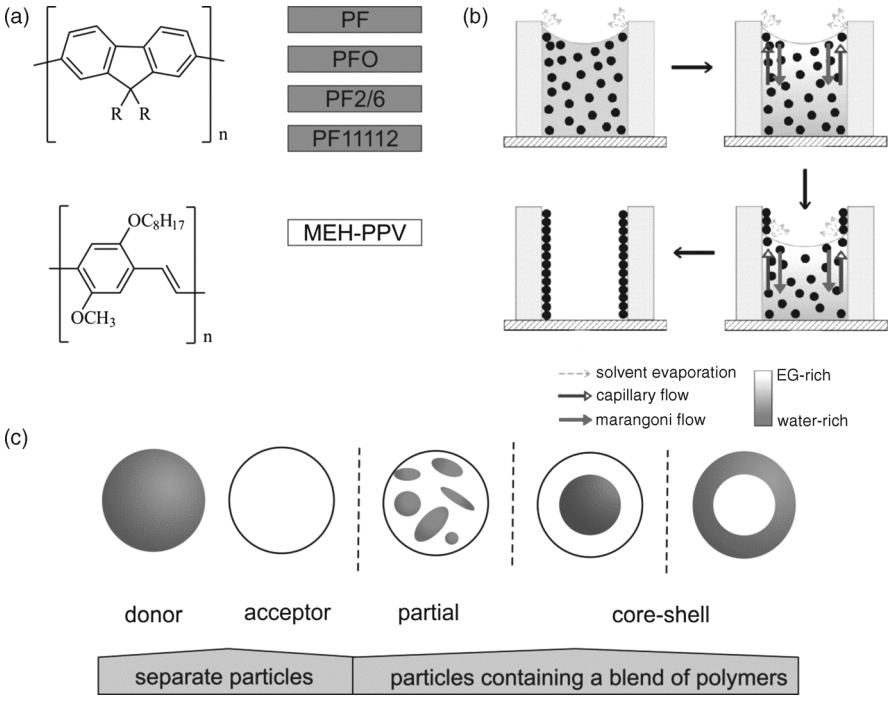

Figure 1.3 (a) Chemical structures of polyfluorenes (PF (R = hexyl), PFO (R = octyl), PF2/6 (R = 2-ethylhexyl), and PF11112 (R = 3,7,11-trimethyldodecyl)) and MEH-PPV. (b) Scheme for the solvent evaporation-induced self-assembly of organic particles on the substrates to form films from an aqueous solution containing ethylene glycol. (Reprinted with permission from Ref. [50]. Copyright 2010, American Chemical Society.) (c) Scheme to illustrate separate, partial, and core–shell nanoparticle structures.

The optical properties of poly(9,9-dihexyl)fluorene (PF) nanoparticle films have been studied in detail [51]. Via a so-called reprecipitation method, a rapid injection into water of a π-conjugated polymer dissolved in THF solution followed by sonication resulted in small nanoparticle (diameter 30 nm) dispersions, prepared without using surfactant. The nanoparticles were drop casted on a substrate to form a thin film and the film thickness was measured with AFM to be 35 nm for the nanoparticles, which corresponds to the diameters of the particles. Remarkably, the fluorescence quantum yield for films of the nanoparticles was $\Phi_{PL} = 68\%$, while drop-casted thin films of PF lacking nanoparticles displayed only a quantum yield in the range of $\Phi_{PL} = 23–44\%$, depending on the film thickness. Interestingly, the redshift in the emission wavelength is greatly reduced for the PF nanoparticle films compared to PF films. Nanoparticles offer an attractive alternative route to fabricate films compared to the conventional solution route since nanoparticles in the film state reveal almost identical properties than in the dispersion [51].

Ordered organic nanoparticle films of PFO and poly[2-methoxy-5-(2′-ethylhexyloxy)-1,4-phenylene vinylene] (MEH-PPV) can be obtained by solvent evaporation-induced self-assembly (Figure 1.3a and b) [50]. By proper introduction of a second solvent such as ethylene glycol into the solution, a so-called Marangoni flow in the opposite direction of the capillary flow can be achieved, counterbalancing the transportation of nanoparticles toward the contact line by the capillary flow (Figure 1.3b) [50]. Consequently, the self-assembly of nanoparticles on the substrate is controlled by the nanoparticle–substrate and nanoparticle–nanoparticle interactions [50]. During the drying process of the solution, a uniform film of the nanoparticles can be achieved on the substrate without any additives. The technique could be an alternative for conventional thin-film processing techniques such as spin coating that require viscous solutions.

1.2.1.3 **OLEDs**

Mixed organic nanoparticles can be prepared either as separate polymer particles or as particles containing a blend of polymers (Figure 1.3c). Tuncel and coworkers constructed different bicomponent nanoparticles, separate, mixed, and core–shell particles, composed of PF as an energy donor and MEH-PPV as an energy acceptor (Figure 1.3) to investigate which morphology resulted in efficient energy transfer [35]. Separate particles are achieved by the preparation of PF and MEH-PPV nanoparticles separately using the reprecipitation method and subsequent mixing. Due to the long distance in solution between donor and acceptor particles, no energy transfer is observed. Mixed particles are made by mixing PF and MEH-PPV prior to nanoparticle formation. In this case, the donor and acceptor polymers are at close distance and energy transfer is observed. Core–shell particles of PF and MEH-PPV were prepared by first injecting one polymer stock solution into water and subsequently adding the second polymer. The formation of core–shell nanoparticles was verified by the observation of energy transfer. Interestingly, the highest energy transfer efficiency (up to 35%) was observed for the core–shell structure in which the PF is located at the periphery of the nanoparticles.

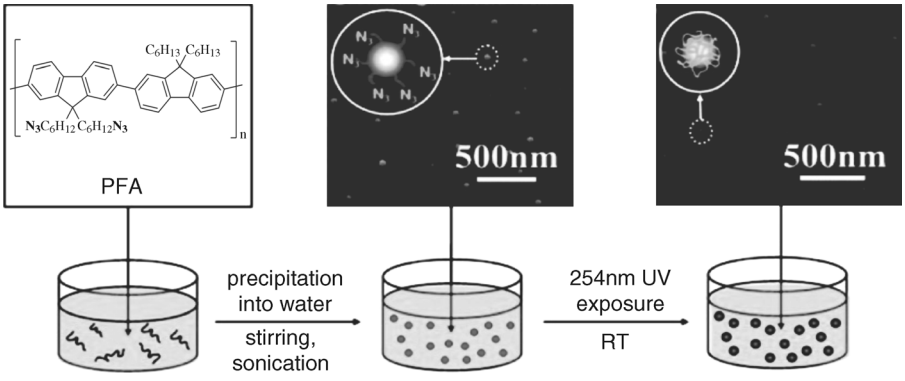

Figure 1.4 Schematic representation of the preparation of the shelled architecture of the conjugated polymer nanoparticles exhibiting white emission. (Reprinted with permission from Ref. [52]. Copyright 2011, American Chemical Society.)

Organic dyes have also been used as energy acceptors in order to tune the emission wavelength of aqueous self-assembled nanoparticles [36]. Negatively charged polyfluorene nanoparticles (PF2/6) made by the miniemulsion method using an ionic surfactant showed effective excitation energy transfer from the nanoparticles to surface-bound cationic fluorescent rhodamine dye. Such studies not only are interesting for tuning the emission wavelength in optoelectronic applications such as OLEDs but could also be interesting for future sensing in water [36]. White-emitting conjugated polymer nanoparticle dispersions have been used for application in OLEDs [52]. Polyfluorene nanoparticles containing azide as cross-linkable group have been made by the reprecipitation method (Figure 1.4). After cross-linking with UV light, mechanically stable particles with a cross-linked shell were obtained in which the core and shell have different energy levels, with the core emitting in the blue and the shell emitting green-yellow [52]. By controlling the shell formation, the energy transfer process between the energy donor core and energy acceptor shell can be tuned to generate white emissive particles. Based on these particles, an OLED could be constructed showing white light electroluminescence.

OLEDs have also been made based on PFO and poly(*p*-phenylene vinylene) (POPPV, Figure 1.5) blended nanoparticles by Foulger and coworkers in which

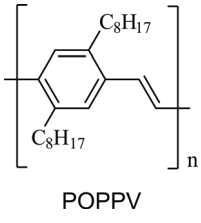

Figure 1.5 Chemical structure of POPPV.

color tuning of the electroluminescence from blue to green was achieved by energy transfer from the PFO energy donor to the POPPV energy acceptor [53]. To the nanoparticle dispersion, a binder (poly(3,4-ethylenedioxythiophene):poly(styrene sulfonate), PEDOT:PSS) was added to prevent electrical shorts before spin coating onto the transparent indium tin oxide (ITO) anode forming the active layer of the OLED (Figure 1.5) [54]. The inherent lack of solubility of POPPV in organic solvents has hampered its application in devices but by creating mixed particles this polymer could be applied in OLEDs [53]. These nanoparticle dispersions can most likely be printed into devices through high-throughput manufacturing techniques (e.g., roll-to-roll printing) [53].

To study the fluorescence of F8BT particles, Barbara and coworkers measured electrogenerated chemiluminescence of single immobilized nanoparticles [55] by using a newly developed single-molecule spectroelectrochemistry technique [56]. Electrochemiluminescence from 25 nm sized immobilized nanoparticles was observed, which shows that this technique serves as a powerful method to obtain information about particle environments [55].

It is well known that the blue emission of polyfluorenes as an emission layer in OLEDs frequently changes into a yellow emission band at 500–550 nm, as a result of fluorenone defects [57–59]. This property has been used to create yellow emissive nanoparticles based on fluorene copolymers in which fluorenone moieties were introduced [60,61]. Nanoparticles could be prepared in aqueous solution of 2,7-poly (9,9-dialkylfluorene-*co*-fluorenone) (PFFO) by the miniemulsion process using cellulose acetate butyrate (CAB) as a surfactant (Figure 1.6a) [60]. Interestingly, nanoparticles with four main size classes, namely, 500, 150, 50, and 5 nm, could be produced showing a size-dependent emission with a yellow to blue color shift (Figure 1.6b). Most likely in the smaller particles, the formation of the yellow excimer emission is suppressed due to reduction of the interaction and order between the polymer chains [60]. The PFFO nanoparticles were revealed to be suitable for inkjet printing and successfully used to print photoluminescent patterns using a very low amount of PFFO (Figure 1.6c) [61]. This nanoparticle suspension shows the properties of inks commonly used in inkjet printing processes as well as being easy to handle and use as a stable, nonhazardous solvent [61].

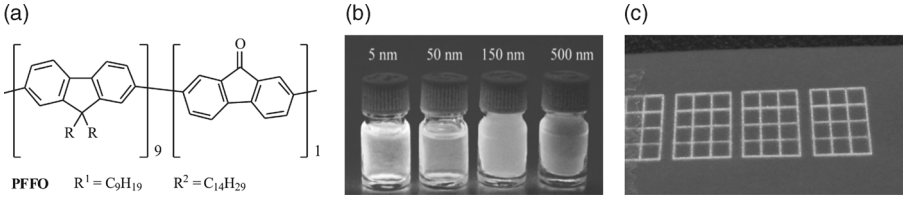

Figure 1.6 (a) Chemical structures of fluorene–fluorenone copolymers used for nanoparticle preparation (R^1 [60]) and inkjet printing (R^2 [61]). (b) Nanoparticle size-dependent emission varying from blue to yellow. (Reprinted with permission from Ref. [54]. Copyright 2008, American Chemical Society.) (c) Inkjet printed patterns under UV light. (Reproduced with permission from Ref. [61].)

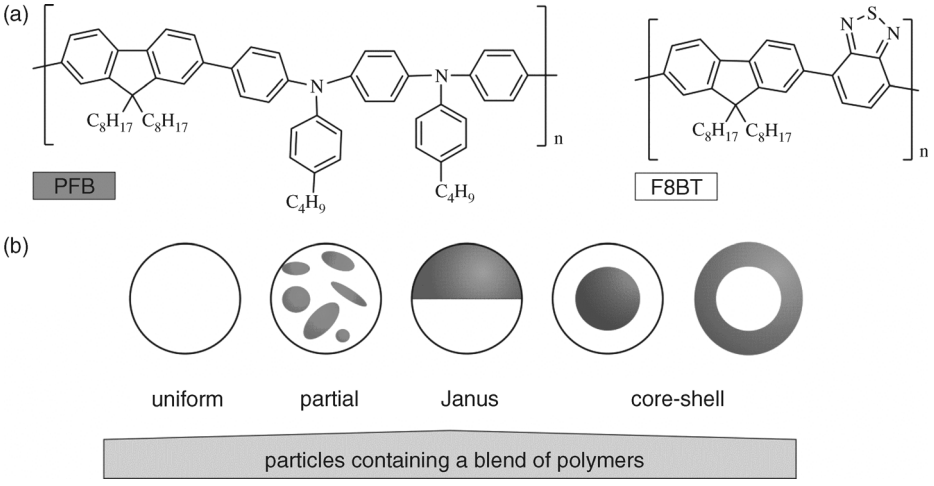

Figure 1.7 (a) Chemical structures of PFB (donor) and F8BT (acceptor). (b) Schematic illustration of the nanomorphology of particles containing a blend of polymers. The mixed nanoparticles could form uniform mixed, partial mixed, Janus-like, or core–shell structures.

1.2.1.4 **Solar Cell Applications**

As we have seen, particles containing a blend of polymers can have different nanomorphologies such as uniform mixed, partial mixed, Janus-like, or core–shell supramolecular structures (Figure 1.7). The nanomorphology of poly(9,9-dioctylfluorene-*co*-bis-*N*,*N*-(4-butylphenyl)-bis-*N*,*N*-phenyl-1,4-phenylenediamine) (PFB) and F8BT nanoparticles containing a blend of polymers (weight ratio 1 : 1) prepared via the miniemulsion method has been extensively studied [32–34]. These polymers were chosen because photoinduced charge transfer occurs between F8BT (electron acceptor) and PFB (electron donor), which is an important process in organic solar cell devices that highly depend on the local environment [62–65]. This intermixing of these two polymers can be studied by interchain exciplex emission. Neher and coworkers investigated thin films of mixed particles by photoluminescence (PL) spectroscopy detecting the presence of PFB-rich and F8BT-rich domains [32]. It was concluded that PFB/F8BT blend nanoparticles form Janus-like structures. Later, direct imaging of these nanoparticles could be achieved by scanning transmission X-ray microscopy (STXM) compositional maps [33]. These studies indicated that these nanoparticles separate into core–shell nanomorphology, with an F8BT-rich core and a PFB-rich shell (Figure 1.7) [33]. Recently, Gao and Grey prepared small (∼58 nm) and large (∼100 nm) PFB/F8BT nanoparticles that were studied by single-particle PL spectroscopy to determine the particle morphology [34]. Size-independent efficient energy transfer from PFB (donor) and F8BT (acceptor) in PFB/F8BT blend nanoparticles was observed but no exciplex emission. These data suggest that the nanoparticles phase segregated in domains with the sizes of ∼20–40 nm [34].

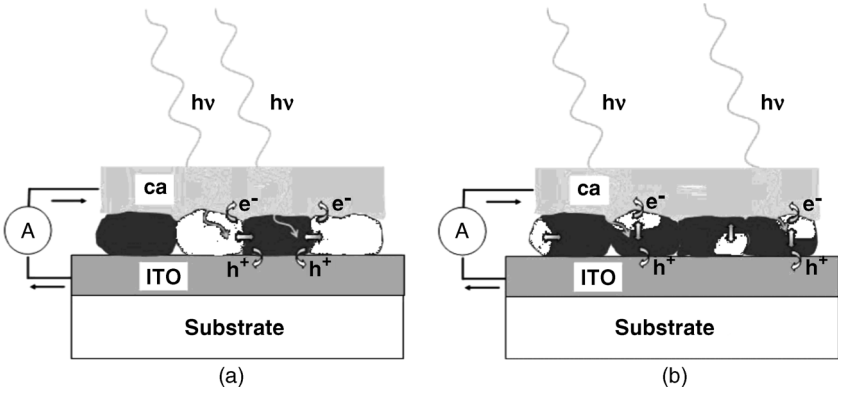

Figure 1.8 Schemes of solar cell devices based on separate particles (a) and a mix of polymers in each particle (b). (Reprinted with permission with Ref. [67]. Copyright 2004, American Chemical Society.)

The first solar cell containing polyfluorene nanoparticles was prepared by Neher and coworkers [66]. PFB (electron donor)/F8BT (electron acceptor) mixed nanoparticles from 1 : 1 weight mixtures in chloroform or xylene were prepared via the miniemulsion method. For the organic solar cells, the polymer dispersions were spin coated onto glass that was covered with transparent ITO electrode. Afterward, the Ca/Al cathode was evaporated onto the particle monolayer. Remarkably, the external quantum efficiency (EQE) was almost unaffected by the solvent from which the particles were synthesized. Furthermore, the efficiency of 1.7% is among the best reported for 1 : 1 weight ratio of PBT/F8BT layers spin coated from xylene, but below the efficiency reported [64] for layers spin coated from chloroform [66]. In a more detailed study, solar cell devices containing separate particles and mixed particles of PFB/F8BT in a weight range of 5 : 1 to 1 : 5 have also been studied (Figure 1.8) [67]. Particles retained their spherical shape after spin coating, leading to low efficiency in the solar cells. Therefore, the spin-coated layers were annealed to 150 °C for 2 h, which led to the flattening of nanoparticles and a more homogeneous surface [67]. Solar cells prepared from annealed separate nanoparticle dispersions showed the highest efficiency of approximately 2% with the highest concentration of PFB (weight ratio 5 : 1). Interestingly, solar cells from mixed PFB/F8BT particles revealed efficiency of up to 4% for F8BT-rich mixed particles (weight ratio 1 : 2). This efficiency is among the highest value reported for PFB/F8BT blended solar cells [64]. The authors propose that the differences between separate and mixed particles in device performance are due to the different dimensions of phase separation in layers of separate or mixed particles (Figure 1.8). In layers of separate particles, the efficiency is determined by the probability that excitons are formed at the interface of two phases and dissociate into free carriers [67]. Due to the rather small exciton diffusion length of the F8BT phase, the F8BT polymer particles need to be surrounded and in direct contact by PFB particles to ensure dissociation of

F8BT excitons [67]. In contrast, the efficiency of solar cells containing both polymers in mixed nanoparticles is determined by the probability that both kinds of charge carriers on a mixed particle can be extracted to the corresponding electrode [67].

Snaith and Friend have developed multilayer structures for OPVs of polymers that are originally soluble in a common solvent by depositing PFB/F8BT (weight ratio 1 : 1) nanoparticles and spin coating them with a thin polymer film of F8BT [68]. Highly uniform films of nanoparticles on ITO glass were obtained by the so-called electroplating method. Unfortunately, the device performance was only 0.4% due to the excess of isolating surfactant blocking charge transfer.

1.2.2 Imaging and Sensing Applications

1.2.2.1 Characterization of Nanoparticles

Nanoparticles in water for imaging and sensing applications are mostly prepared by the reprecipitation method in which a π-conjugated polymer dissolved in THF solution is rapidly injected into water and subsequently sonicated [30,31]. During nanoparticle formation, a competition exists between aggregation and chain collapse of the π-conjugated polymers. Therefore, the size of the nanoparticles, from a few nm (a single, collapsed conjugated polymer chain) to 50 nm, can be controlled by the polymer concentration in THF solution [69]. For example, F8BT nanoparticles possess a diameter of around 10 nm after injection of a diluted stock solution and around 25 nm after injection of a concentrated stock solution [70]. The absorption of the nanoparticles is usually blueshifted compared to a solution of the polymer in a good solvent due to an overall decrease in conjugation length upon nanoparticle formation (Figure 1.9). The fluorescence spectra of the nanoparticles

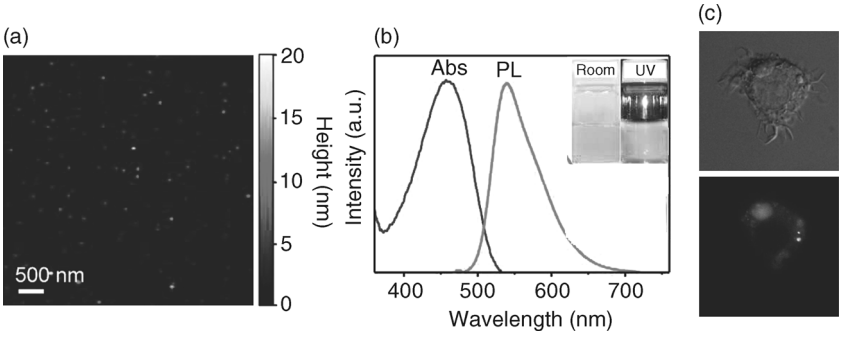

Figure 1.9 (a) AFM image of F8BT nanoparticles. (b) The absorption and emission ($\lambda_{ex} = 475$ nm) spectra of F8BT nanoparticles suspended in water. The inset shows the nanoparticles suspended in water under room light and UV light illumination. (Reprinted with permission from Ref. [71]. Copyright 2009, American Chemical Society.) (c) Differential interference contrast (DIC) image (top) and fluorescence image (bottom) of macrophage cells with F8BT. (Reprinted with permission from Ref. [70]. Copyright 2008, American Chemical Society.)

exhibit mainly a redshift and a long red tail because of interchain interaction due to the chain collapse of the π-conjugated polymer [70]. The nanoparticles exhibit an excellent photostability and extraordinary fluorescent brightness in comparison to organic dyes, quantum dots, or dye-loaded particles [70]. An estimate of the fluorescent brightness is given by the product of the peak absorption cross section and the fluorescence quantum yield; the quantum yield of PFO nanoparticles is up to 40% and for F8BT nanoparticles it is 7% with an absorption cross section 10–100 times larger than that of CdSe quantum dots [70]. π-Conjugated polymer nanoparticles also have the largest two-photon action cross section reported for particles of comparable size representing their potential for multiphoton fluorescence microscopy [69]. In addition, intracellular particle tracking is demonstrated for F8BT showing the capability of nanoparticles to measure the nanoscale motion of individual biomolecules [71]. In case of PFO nanoparticles, the addition of organic solvent led to solvent-induced swelling and a phase transition from a glassy phase, which is kinetically trapped during nanoparticle formation, to the β-phase, which exhibits a narrow, redshifted fluorescence and increased quantum yield, takes place [72,73]. In order to control the supramolecular organization in fluorene-based nanoparticles, block copolymers and amphiphilic polymers have also been synthesized [74–82].

1.2.2.2 **Biosensing**

Energy transfer in conjugated polymer nanoparticles has been studied extensively to improve their quantum efficiency and tune their emission color [5]. McNeill and coworkers prepared polymer nanoparticle blends of the blue-emitting PF doped with green-, yellow-, and red-emitting polymers (poly[{9,9-dioctyl-2,7-divinylenefluorenylene}-*alt*-*co*-{2-methoxy-5-(2-ethylhexyloxy)-1,4-phenylene}] (PFPV), F8BT, and MEH-PPV, respectively) (Figure 1.10a) [83]. These particles containing a blend of two polymers were prepared by adding a mixture of the two polymers dissolved in THF into water yielding mixed particles with a size of around 25 nm. The donor emission of PF was almost completely quenched by an acceptor incorporation of 6 wt% revealing high energy transfer efficiencies. Furthermore, this indicates a uniform blend mixture in the nanoparticles (Figure 1.6), which could be due to kinetic trapping during nanoparticle formation [83]. McNeill and coworkers also reported fluorescent dye-doped nanoparticles [84]. PF nanoparticles were doped with blue- (perylene), green- (coumarin 6), orange- (Nile red), and red-emitting (TPP) dyes. The emission of PF nanoparticles was almost completely quenched after incorporation of a low percentage of dye (2–5 wt%) (Figure 1.10b) [84]. Recently, Chiu and coworkers developed near-infrared emitting nanoparticles by doping F8BT polymer nanoparticles with a near-infrared dye [85]. All dye-doped nanoparticles showed a much higher photostability and better fluorescence brightness than single dyes in solution, which points out the potential of these nanoparticles in bioimaging and sensing applications.

Photoswitchable fluorescent nanoparticles can be created by using energy transfer from the conjugated polymer PFPV or MEH-PPV to a photochromic diarylethene dye [86]. The photochromic dye has no effect on the nanoparticle emission in its

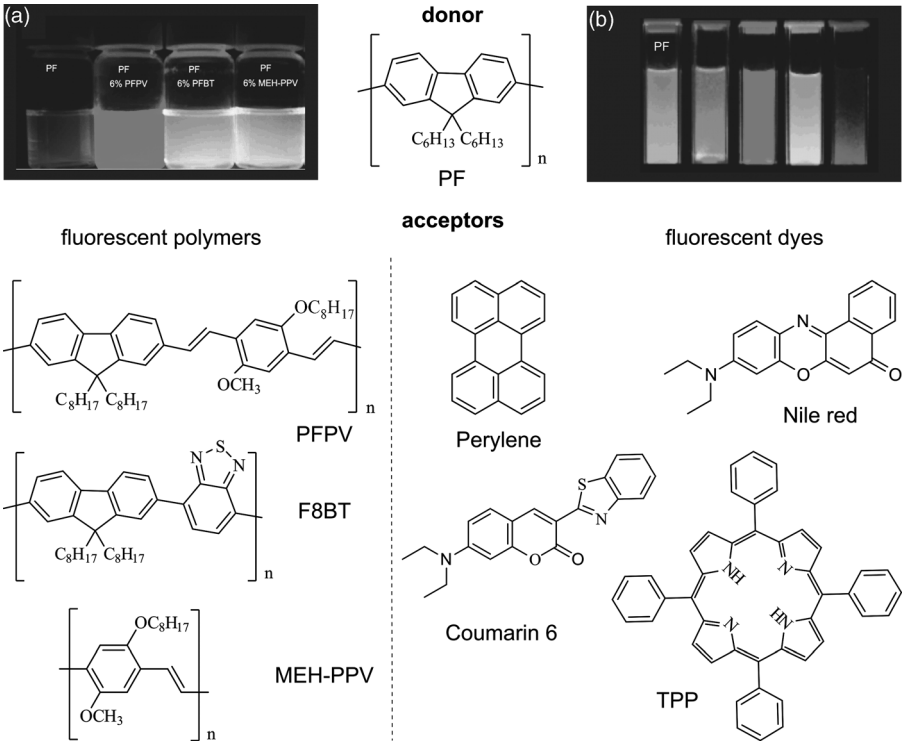

Figure 1.10 (a) Photographs of fluorescence emission from aqueous solution of PF nanoparticles doped with PFPV, F8BT, and MEH-PPV (from left to right) taken under a UV lamp (365 nm) and the chemical structures of the polymers (bottom). (Reprinted with permission from Ref. [83]. Copyright 2006, American Chemical Society.) (b) Photographs of fluorescence emission from aqueous solution of PF nanoparticles doped with perylene, coumarin 6, Nile red, and TPP (from left to right) taken under a UV lamp (365 nm) and the chemical structures of the dyes (bottom). (Reprinted with permission from Ref. [84]. Copyright 2008, American Chemical Society.)

closed form, but quenches the emission of the nanoparticles in its open form after switching with UV light. A given fluorophore can be localized with high precision if neighboring fluorophores are switched "off" at the time of the imaging. Therefore, photoswitchable fluorescent nanoparticles hold great promise in super-resolution fluorescence imaging [86,87].

Energy transfer processes in conjugated polymer nanoparticles can also be exploited to develop an oxygen and a temperature sensor for biological imaging (Figure 1.11) [37,38]. Oxygen sensing in living cells is highly relevant in biology and medicine as the oxygen level in cells varies with respect to various diseases, for example, cancer [88,89]. The π-conjugated polymer nanoparticles containing PF or PFO were doped with an oxygen-sensitive phosphorescent dye (platinum(II) octaethylporphyrin (PtOEP)) [37]. The phosphorescence from PtOEP is very sensitive to oxygen and therefore quenched in an oxygen-saturated solution.

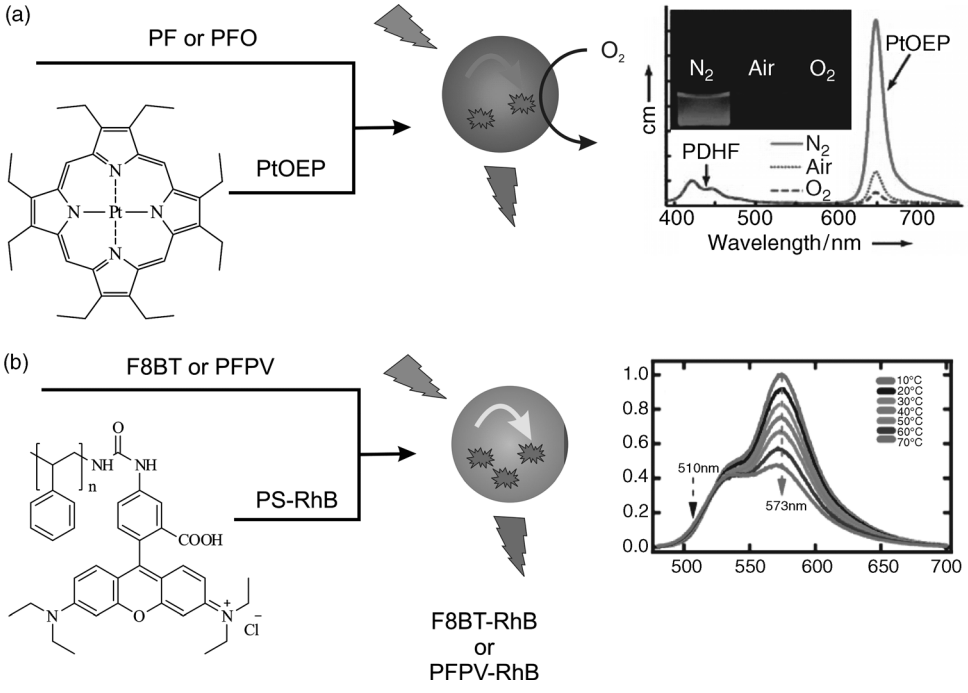

Figure 1.11 (a) Schematic illustration of polymer nanoparticles for oxygen sensing (left). Oxygen-dependent emission spectra of the 10% PtOEP-doped PF dots (right). (Reprinted with permission from Ref. [37].) (b) Schematic illustration of the polymer nanoparticles (F8BT–RhB or PFPV–RhB) for temperature sensing (left). Temperature-dependent emission spectra of F8BT–RhB nanoparticles (right). (Reprinted with permission from Ref. [38]. Copyright 2011, American Chemical Society.)

Upon incorporation of 10 wt% PtOEP into PF or PFO, the nanoparticles exhibit significantly reduced donor fluorescence and a strong red emission from PtOEP, revealing energy transfer from the fluorene polymer to PtOEP (Figure 1.11a). The nanoparticles show 1000 times higher brightness than conventional oxygen dyes due to both efficient light harvesting by the polymer nanoparticles and efficient energy transfer from the polymer to the dye. The dye-doped nanoparticles were taken up by macrophage cells and showed no cytotoxicity or phototoxicity during incubating and imaging indicating their potential for quantitative mapping of local molecular oxygen levels in living cells [37]. In the next step, a local temperature sensor in living cells based on F8BT and PFPV nanoparticles doped with a temperature-sensitive dye was developed (Figure 1.11) [38]. Cancer cells can be at higher temperatures compared to healthy cells due to different cellular metabolism, so the development of temperature sensors in cells is significant [90]. The temperature-sensitive dye rhodamine B (RhB) was attached to polystyrene, and the resulting polymer was mixed with F8BT or PFPV and dispersed into water, yielding stable, bright, and temperature-sensitive nanoparticles (F8BT–RhB or PFPV–RhB). Efficient energy transfer was observed from F8BT or PFPV to RhB, whose emission

intensity decreased linearly with increasing temperature in the physiologically relevant range. Furthermore, the nanoparticles were successfully taken up by HeLa cells showing lower red fluorescence intensity at 36.5 °C than at 13.5 °C indicating their potential for highly parallelized and spatiotemporally resolved temperature measurements in cells [38]. In another study, π-conjugated polymer nanoparticles could be exploited in chemical sensing using a solid film of separate MEH-PPV and PFO nanoparticles [91]. Free hydroxyl radicals and sulfate anion radicals could be detected by a change in PFO solid-state fluorescence. Solid-state detection is highly desirable for off-site laboratory detection since solid-state samples are easy to store, handle, and transport [91].

1.2.2.3 **Bioimaging**

In the first reports of π-conjugated polymer nanoparticles, it was shown that these particles are unspecifically taken up via endocytosis by the cell [70]. In contrast, for targeted bioimaging with nanoparticles, control over surface chemistry and conjugation to ligands or biomolecules is crucial [4]. The functionalization of fluorene-based nanoparticles for bioimaging and sensing is challenging. Nanoparticles prepared by *in situ* polymerization in water with the miniemulsion method are also compatible with living cells and suitable as ultrabright probes for cellular imaging and therefore opening an approach for accessing structured nanoparticles, for example, with a functional interior or exterior [92–94]. Moreover, functionalization and stabilization of π-conjugated polymers can be achieved by applying the click reaction in water with azide-functionalized fluorene polymers [95]. Another potential route to biofunctionalization was demonstrated by capping or entwining fluorene-based nanoparticles with poly(ethylene glycol) (PEG) [96]. PEG is an important agent for biological applications of nanoparticles as it is nontoxic, approved for human use, and significantly reduces nonspecific binding to biomacromolecules [97,98]. Another strategy to reach surface-functionalized polymer nanoparticles was shown by encapsulation of the nanoparticles into PEG lipids [99,100]. As PEG lipids are commercially available, surface modification of conjugated polymer nanoparticles with functionalized PEG lipids is a feasible method to create hydrophilic biocompatible nanoparticles. This strategy was further used to synthesize magnetic–fluorescent nanoparticles by encapsulation of π-conjugated polymer nanoparticles and superparamagnetic iron oxides into PEG lipid micelles [101]. Furthermore, the π-conjugated polymer nanoparticles can be encapsulated into silica allowing the attachment of functional groups for bioconjugation at the silica surface [30,102].

The incorporation of different polymeric matrices during the nanoparticle preparation is an efficient and feasible method to synthesize nanoparticles with functional groups on their surface leading to biocompatible and surface-functionalized nanoparticles that were specifically taken up by cells via receptor-mediated endocytosis [103,104].

This method was exploited by Chiu and coworkers leading to *in vitro* specific cellular targeting and *in vivo* tumor targeting (Figure 1.12) [105–107]. Mixing F8BT with an amphiphilic polymer (poly(styrene-*co*-maleic anhydride), PSMA) yielded

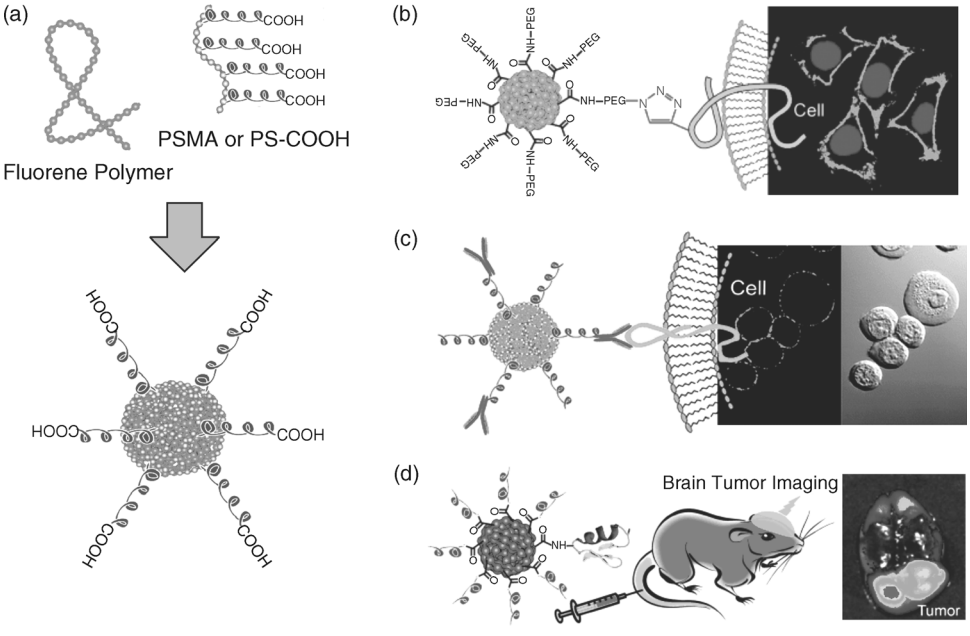

Figure 1.12 (a) Schematic representation of the preparation of carboxyl-functionalized polymer nanoparticles. (Reprinted with permission from Ref. [106]. Copyright 2010, American Chemical Society.) (b) Bioorthogonal labeling of cellular targets using polymer nanoparticles and click chemistry. (Reproduced with permission from Ref. [105].) (c) Polymer nanoparticle bioconjugates for specific cellular targeting. (Reprinted with permission from Ref. [106]. Copyright 2010, American Chemical Society.) (d) Polymer nanoparticle bioconjugates for *in vivo* tumor targeting. (Reproduced with permission from Ref. [107].)

bright nanoparticles with carboxyl groups on the surface that can be used for further surface functionalization (Figure 1.12a) [105]. In the first approach, small ligands such as amino-azide, amino-alkyne, or amino-PEG were attached to the surface (Figure 1.12b). The surface-functionalized nanoparticles revealed a similar diameter to F8BT nanoparticles and could be employed in specific cellular labeling. The cells were metabolically labeled with azide- or alkyne-bearing artificial amino acids. Click chemistry could be successfully exploited to observe a bright fluorescence of the labeled cell membrane at very low concentrations of nanoparticles (Figure 1.12c) [105]. Similar surface carboxylated nanoparticles, using a polystyrene polymer PS–PEG–COOH and F8BT, were used to covalently link biomolecules such as streptavidin and immunoglobulin (IgG) to the fluorescent particles (Figure 1.12c) [106]. These surface-functionalized nanoparticles were exploited to specifically and effectively label cellular targets such as cell surface marker in breast cancer cells with no unspecific binding. Furthermore, the nanoparticles showed much higher fluorescence brightness than commonly used dyes or quantum dots. These results show that successful functionalization of small ligands and biomolecules opens a variety of fluorescence-based biological applications for these bright nanoparticles.

Furthermore, carboxyl-functionalized F8BT nanoparticles could be used as a fluorescent probe for sensitive Cu^{2+} and Fe^{2+} detection [108]. These ions were chelated by the carboxyl moieties, and therefore, aggregation and quenching of the F8BT nanoparticles was observed.

To apply fluorescent polymer nanoparticles for *in vivo* targeting, high fluorescence brightness in the near-infrared region needs to be achieved to overcome scattering, absorption, and autofluorescence from tissues. Second, nanoparticles must be specifically delivered to the diseased tissue *in vivo*. Based on F8BT nanoparticles doped with an efficient red-emitting polymer, a fluorescent probe that is 15 times brighter than commercial quantum dots in the near-infrared region was developed [107]. The polymer blend had a high absorption cross section in the visible range and a high quantum yield (56%) in the deep red ($\lambda_{em} = 650$ nm) emission region. The nanoparticles were functionalized with PSMA to generate surface carboxyl groups to covalently attach a tumor-specific targeting peptide ligand (CTX). After injection in the tail vein of a mouse, the nanoparticle–CTX conjugate successfully traversed the blood–brain barrier and specifically targeted a mouse brain tumor as shown by biophotonic imaging, biodistribution, and histological analyses (Figure 1.12d) [107].

1.3 Nanoparticles Based on Fluorene Oligomer

1.3.1 Characterization

Fluorene-based oligomers are also capable of forming spherical assemblies in water for optoelectronic and biological applications. Recently, white light emitting nanoparticles in aqueous solution have been reported that are fabricated by a very simple method [109,110]. Oligofluorene derivatives are molecularly dissolved in THF and self-assemble to stable nanoparticles upon injection of this THF solution into water, producing a blue emission. By simply mixing with a red-orange emitting dye (DCM) in THF, energy transfer is observed in water generating white emissive oligomer nanoparticles (Figure 1.13a) [110].

In another approach, vesicle-like nanospheres spanning the emission spectra from blue to red were observed in THF using different oligofluorene derivatives (Figure 1.13b) [111]. Different colors, including white emission, were observed by again simply mixing the fluorene oligomers. Nanoparticles based on oligofluorenes were also prepared by Tagawa and coworkers [112] and Yang and coworkers [113] showing a pure green emission of the fluorene nanoparticles in a water–THF mixture.

Recently, bolaamphiphile fluorene oligomers forming fluorescent organic nanoparticles with emission wavelengths spanning the entire visible spectrum, showing even white emission, were synthesized (Figure 1.14a) [109]. The π-conjugated oligomer is built up of two fluorene moieties connected by different aromatic cores. The particles show excellent quantum yields in water, up to 70% for the

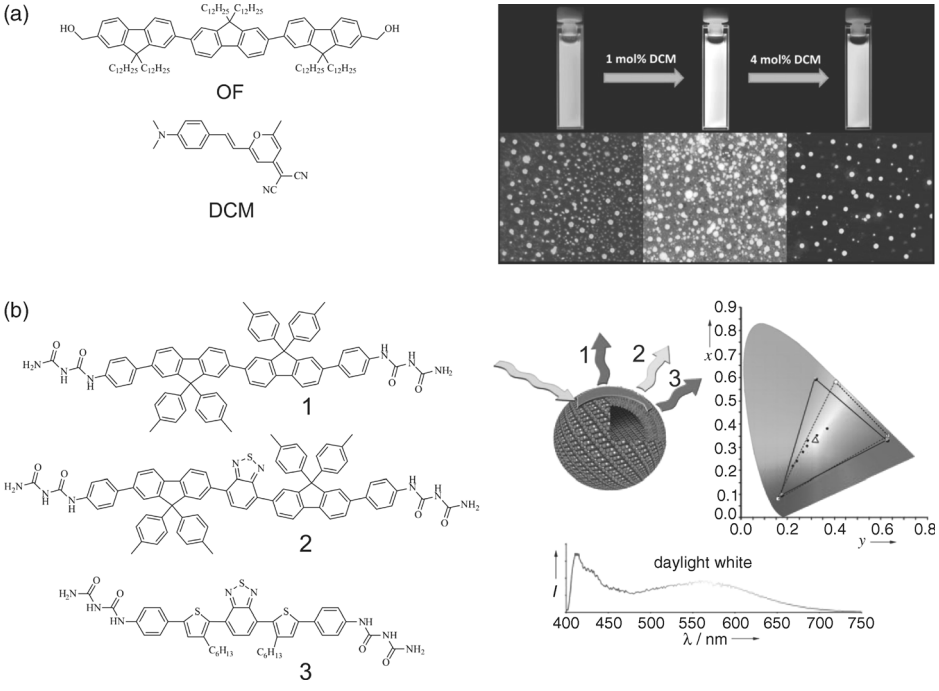

Figure 1.13 (a) Chemical structure of the oligofluorene derivative OF and the dye DCM (left). Photographs of the nanoparticles in aqueous solution with different amounts of DCM and the corresponding fluorescence microscope images (right). (Reproduced with permission from Ref. [110].) (b) Chemical structures of the oligofluorene derivatives (left) that spontaneously form vesicles in THF. Energy migration in tricomponent spherical aggregates allows a large fraction of the visible spectrum to be covered (right). Open circles correspond to the chromatic coordinates of the emission from the vesicles and define a gamut (dashed line) of available colors. Filled circles represent the color obtained by doping the vesicles. For comparison, the gamut of a standard RGB display is also shown (solid lines). Emission spectrum of a single vesicle-like aggregate emitting white light (right bottom). (Reproduced with permission from Ref. [111].)

benzothiadiazole core containing derivative. Separate particles could be observed by fluorescence microscopy while mixed particles showed very efficient energy transfer and appropriate mixing resulted in a white emission spectrum. The absence of exchange of molecules between particles, good stability, variability of emission, and high quantum yields provide the possibility of these particles to be employed in multitarget labeling.

1.3.2
Nanoparticles for Sensing and Imaging

An amphiphilic benzothiadiazole derivative was functionalized with ligands, either mannose or azide, at the wedge of the molecules (Figure 1.14b) [114]. The oligomers functionalized with mannose formed stable, fluorescent nanoparticles in water that

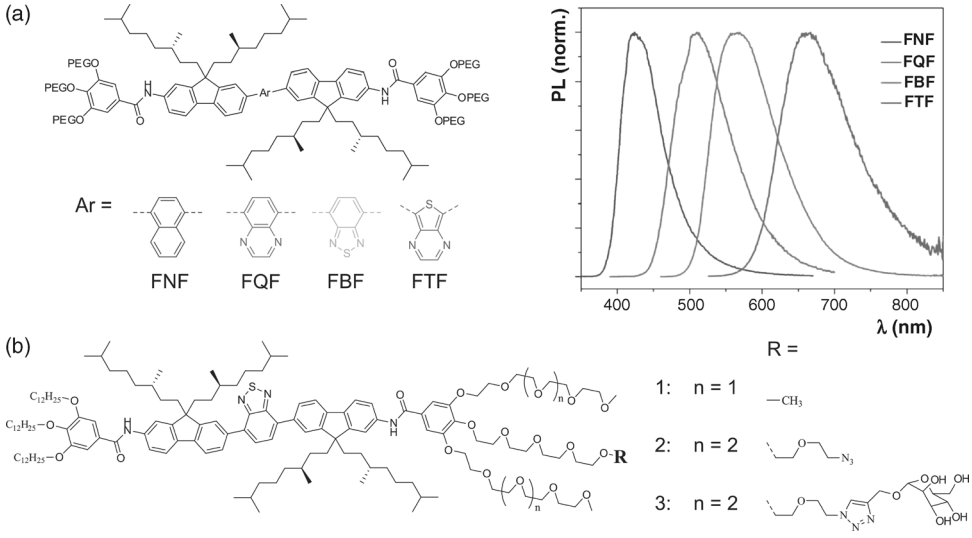

Figure 1.14 (a) Chemical structure of bolaamphiphilic fluorene derivatives (PEG = tetraethylene glycol, left). Photoluminescence spectra in water of the fluorene-based bolaamphiphiles (right). (Reproduced with permission from Ref. [109]. Copyright 2009, the Royal Society of Chemistry.) (b) Chemical structure of the functionalized fluorene-based amphiphiles. Reproduced with permission from Ref. [114].

showed specific binding to concanavalin A. The azide nanoparticles could be postfunctionalized with mannose and biotin exploiting click chemistry. The nanoparticles functionalized with biotin showed efficient energy transfer to dye-labeled streptavidin, while the postfunctionalized mannose nanoparticles showed much less energy transfer than prefunctionalized particles. Nanoparticles for dual targeting were developed by mixing the azide- and mannose-functionalized fluorene oligomers in THF forming mannose particles with also azide ligands. The click reaction was applied to these particles yielding particles that show binding to concanavalin A and streptavidin. This result represents new approach with high applicability to multitargeted imaging and sensing.

Very recently, fluorene oligomers bearing an azide ligand for further functionalization on the fluorene moiety that forms stable nanoparticles in water have also been prepared [115].

1.4 Conclusions and Perspectives

As can be concluded from this chapter, fluorene-based nanoparticles are attractive systems for optoelectronic devices and sensing and bioimaging applications. A variety of fluorene-based polymers and oligomers have been reported that self-assemble into highly fluorescent nanoparticles in water. The emission wavelength of

the nanoparticles can be easily controlled by the chemical structure of the π-conjugated segment and (partial) energy transfer can also be exploited to reach even white emission. Stable nanoparticles can be prepared by simple preparation methods that enable printing, which allows the fabrication of large-area patterned electronics in which the nanomorphology of the particles is preserved in the active layer. The use of aqueous self-assembled systems permits the construction of multilayer structures composed of layers formed from an organic solvent and layers formed by deposition of aqueous polymer nanoparticles. For optoelectronic applications, nanoparticles were synthesized mainly by the miniemulsion process and contained surfactants that can limit the device performance. Nanoparticles serve as excellent model systems to study structure–property relationships that are crucial to improve device performance. Remarkably, nanoparticles have not been applied in nanosized optoelectronic devices. It would be interesting to see if spherical assemblies can be used instead of fibers and wires [116].

Nanoparticles based on fluorenes show an extraordinary brightness and excellent photostability compared to single dyes and inorganic nanoparticles. Therefore, these nanoparticles are attractive probes for sensing and cellular and *in vivo* imaging. Nanoparticles could be successfully functionalized with bioligands, but have not yet been applied to either cellular or *in vivo* imaging. As particles based on oligomers are likely adaptive assemblies, they are excellent candidates to study dynamic processes that could mimic lateral diffusion across natural membranes for receptor clustering and enhanced receptor–ligand interactions.

From this chapter it can be concluded that despite numerous challenges, fluorescent nanoparticles based on π-conjugated polymers and oligomers are promising candidates for optoelectronic devices and sensing and imaging applications, and offer great opportunities to push the development of organic nanoparticles toward advanced nanotechnologies.

Acknowledgments

We would like to acknowledge all of our former and current colleagues for the many discussions and contributions. Their names are given in the cited references. We thank M.G. Debije and N. Herzer for their critical reading. Our research has been supported by the Netherlands Organization for Scientific Research (NWO).

References

1 Kaeser, A. and Schenning, A.P.H.J. (2010) Fluorescent nanoparticles based on self-assembled π-conjugated systems. *Adv. Mater.*, **22**, 2985–2997.

2 Tuncel, D. and Demir, H.V. (2010) Conjugated polymer nanoparticles. *Nanoscale*, **2** (4), 484–494.

3 Pecher, J. and Mecking, S. (2010) Nanoparticles of conjugated polymers. *Chem. Rev.*, **110** (10), 6260–6279.

4 Li, K. and Liu, B. (2011) Polymer encapsulated conjugated polymer nanoparticles for fluorescence

bioimaging. *J. Mater. Chem.*, **22** (4), 1257–1264.
5 Tian, Z., Yu, J., Wu, C., Szymanski, C., and McNeill, J. (2010) Amplified energy transfer in conjugated polymer nanoparticle tags and sensors. *Nanoscale*, **2** (10), 1999–2011.
6 Asawapirom, U., Bulut, F., Farrell, T., Gadermaier, C., Gamerith, S., Güntner, R., Kietzke, T., Patil, S., Piok, T., Montenegro, R., Stiller, B., Tiersch, B., Landfester, K., List, E.J.W., Neher, D., Sotomayor Torres, C., and Scherf, U. (2004) Materials for polymer electronics applications – semiconducting polymer thin films and nanoparticles. *Macromol. Symp.*, **212** (1), 83–92.
7 Suk, J. and Bard, A. (2011) Electrochemistry and electrogenerated chemiluminescence of organic nanoparticles. *J. Solid State Electrochem.*, **15** (11), 2279–2291.
8 Burroughes, J.H., Bradley, D.D.C., Brown, A.R., Marks, R.N., Mackay, K., Friend, R.H., Burns, P.L., and Holmes, A.B. (1990) Light-emitting diodes based on conjugated polymers. *Nature*, **347** (6293), 539–541.
9 Kulkarni, A.P., Tonzola, C.J., Babel, A., and Jenekhe, S.A. (2004) Electron transport materials for organic light-emitting diodes. *Chem. Mater.*, **16** (23), 4556–4573.
10 Bundgaard, E. and Krebs, F.C. (2007) Low band gap polymers for organic photovoltaics. *Sol. Energy Mater. Sol. Cells*, **91** (11), 954–985.
11 Torsi, L., Cioffi, N., Di Franco, C., Sabbatini, L., Zambonin, P.G., and Bleve-Zacheo, T. (2001) Organic thin film transistors: from active materials to novel applications. *Solid State Electron.*, **45** (8), 1479–1485.
12 Scherf, U. and List, E.J. (2002) Semiconducting polyfluorenes – towards reliable structure–property relationships. *Adv. Mater.*, **14** (7), 477–487.
13 Chen, P., Yang, G., Liu, T., Li, T., Wang, M., and Huang, W. (2006) Optimization of opto-electronic property and device efficiency of polyfluorenes by tuning structure and morphology. *Polym. Int.*, **55** (5), 473–490.
14 Dennler, G., Scharber, M.C., and Brabec, C.J. (2009) Polymer–fullerene bulk-heterojunction solar cells. *Adv. Mater.*, **21** (13), 1323–1338.
15 Chen, J.-T. and Hsu, C.-S. (2011) Conjugated polymer nanostructures for organic solar cell applications. *Polym. Chem.*, **2** (12), 2707–2722.
16 Zhang, J., Campbell, R.E., Ting, A.Y., and Tsien, R.Y. (2002) Creating new fluorescent probes for cell biology. *Nat. Rev. Mol. Cell Biol.*, **3** (12), 906–918.
17 Weissleder, R. (2001) A clearer vision for *in vivo* imaging. *Nat. Biotechnol.*, **19** (4), 316–317.
18 Helmchen, F. and Denk, W. (2005) Deep tissue two-photon microscopy. *Nat. Methods*, **2** (12), 932–940.
19 Patterson, G., Davidson, M., Manley, S., and Lippincott-Schwartz, J. (2010) Superresolution imaging using single-molecule localization. *Annu. Rev. Phys. Chem.*, **61** (1), 345–367.
20 Neher, D. (2001) Polyfluorene homopolymers: conjugated liquid-crystalline polymers for bright blue emission and polarized electroluminescence. *Macromol. Rapid Commun.*, **22** (17), 1365–1385.
21 Abbel, R., Schenning, A.P.H.J., and Meijer, E.W. (2009) Fluorene-based materials and their supramolecular properties. *J. Polym. Sci. Part A: Polym. Chem.*, **47** (17), 4215–4233.
22 Scherf, U. and Neher, D. (eds) (2008) *Polyfluorenes*, Advances in Polymer Science, vol. 212, Springer, Berlin, pp. 1–322.
23 Leclerc, M. (2001) Polyfluorenes: twenty years of progress. *J. Polym. Sci. Part A: Polym. Chem.*, **39** (17), 2867–2873.
24 Beaupré, S., Boudreault, P.T., and Leclerc, M. (2010) Solar-energy production and energy-efficient lighting: photovoltaic devices and white-light-emitting diodes using poly(2,7-fluorene), poly(2,7-carbazole), and poly(2,7-dibenzosilole) derivatives. *Adv. Mater.*, **22** (8), E6–E27.
25 Grimsdale, A. and Müllen, K. (2006) Polyphenylene-type emissive materials: poly(*para*-phenylene)s, polyfluorenes, and ladder polymer. *Adv. Polym. Sci.*, **199**, 1–82.

26 Inganäs, O., Zhang, F., and Andersson, M.R. (2009) Alternating polyfluorenes collect solar light in polymer photovoltaics. *Acc. Chem. Res.*, **42** (11), 1731–1739.

27 Landfester, K. (2009) Miniemulsion polymerization and the structure of polymer and hybrid nanoparticles. *Angew. Chem., Int. Ed.*, **48** (25), 4488–4507.

28 Landfester, K. (2006) Synthesis of colloidal particles in miniemulsions. *Annu. Rev. Mater. Res.*, **36** (1), 231–279.

29 Landfester, K., Schork, F.J., and Kusuma, V.A. (2003) Particle size distribution in mini-emulsion polymerization. *C. R. Chim.*, **6** (11–12), 1337–1342.

30 Wu, C., Szymanski, C., and McNeill, J. (2006) Preparation and encapsulation of highly fluorescent conjugated polymer nanoparticles. *Langmuir*, **22** (7), 2956–2960.

31 Vauthier, C. and Bouchemal, K. (2008) Methods for the preparation and manufacture of polymeric nanoparticles. *Pharm. Res.*, **26** (5), 1025–1058.

32 Kietzke, T., Neher, D., Kumke, M., Ghazy, O., Ziener, U., and Landfester, K. (2007) Phase separation of binary blends in polymer nanoparticles. *Small*, **3** (6), 1041–1048.

33 Burke, K.B., Stapleton, A.J., Vaughan, B., Zhou, X., Kilcoyne, A.L.D., Belcher, W.J., and Dastoor, P.C. (2011) Scanning transmission X-ray microscopy of polymer nanoparticles: probing morphology on sub-10nm length scales. *Nanotechnology*, **22** (26), 265710.

34 Gao, J. and Grey, J.K. (2012) Spectroscopic studies of energy transfer in fluorene co-polymer blend nanoparticles. *Chem. Phys. Lett.*, **522**, 86–91.

35 Ozel, I.O., Ozel, T., Demir, H.V., and Tuncel, D. (2010) Non-radiative resonance energy transfer in bi-polymer nanoparticles of fluorescent conjugated polymers. *Opt. Express*, **18** (2), 670–684.

36 Grigalevicius, S., Forster, M., Ellinger, S., Landfester, K., and Scherf, U. (2006) Excitation energy transfer from semi-conducting polymer nanoparticles to surface-bound fluorescent dyes. *Macromol. Rapid Commun.*, **27** (3), 200–202.

37 Wu, C., Bull, B., Christensen, K., and McNeill, J. (2009) Ratiometric single-nanoparticle oxygen sensors for biological imaging. *Angew. Chem., Int. Ed.*, **48** (15), 2741–2745.

38 Ye, F., Wu, C., Jin, Y., Chan, Y.-H., Zhang, X., and Chiu, D.T. (2011) Ratiometric temperature sensing with semiconducting polymer dots. *J. Am. Chem. Soc.*, **133** (21), 8146–8149.

39 Valeur, B. (2001) *Molecular Fluorescence: Principles and Applications*, Wiley-VCH Verlag GmbH, Weinheim.

40 Thomas, S.W., Joly, G.D., and Swager, T. M. (2007) Chemical sensors based on amplifying fluorescent conjugated polymers. *Chem. Rev.*, **107** (4), 1339–1386.

41 Swager, T.M. (1998) The molecular wire approach to sensory signal amplification. *Acc. Chem. Res.*, **31** (5), 201–207.

42 Duarte, A., Pu, K.-Y., Liu, B., and Bazan, G.C. (2010) Recent advances in conjugated polyelectrolytes for emerging optoelectronic applications. *Chem. Mater.*, **23** (3), 501–515.

43 Pu, K.-Y. and Liu, B. (2011) Fluorescent conjugated polyelectrolytes for bioimaging. *Adv. Funct. Mater.*, **21** (18), 3408–3423.

44 Pich, A.Z. and Adler, H.P. (2007) Composite aqueous microgels: an overview of recent advances in synthesis, characterization and application. *Polym. Int.*, **56** (3), 291–307.

45 Knopp, D., Tang, D., and Niessner, R. (2009) Bioanalytical applications of biomolecule-functionalized nanometer-sized doped silica particles. *Anal. Chim. Acta*, **647** (1), 14–30.

46 Baier, M.C., Huber, J., and Mecking, S. (2009) Fluorescent conjugated polymer nanoparticles by polymerization in miniemulsion. *J. Am. Chem. Soc.*, **131** (40), 14267–14273.

47 Tong, Q., Krumova, M., and Mecking, S. (2008) Crystalline polymer ultrathin films from mesoscopic precursors. *Angew. Chem., Int. Ed.*, **47** (24), 4509–4511.

48 Landfester, K., Montenegro, R., Scherf, U., Güntner, R., Asawapirom, U., Patil, S., Neher, D., and Kietzke, T. (2002) Semiconducting polymer nanospheres in aqueous dispersion prepared by a

miniemulsion process. *Adv. Mater.*, **14** (9), 651–655.

49 Piok, T., Plank, H., Mauthner, G., Gamerith, S., Gadermaier, C., Wenzl, F. P., Patil, S., Montenegro, R., Bouguettaya, M., Reynolds, J.R., Scherf, U., Landfester, K., and List, E.J.W. (2005) Solution processed conjugated polymer multilayer structures for light emitting devices. *Jpn. J. Appl. Phys.*, **44** (1B), 479–484.

50 Zheng, C., Xu, X., He, F., Li, L., Wu, B., Yu, G., and Liu, Y. (2010) Preparation of high-quality organic semiconductor nanoparticle films by solvent-evaporation-induced self-assembly. *Langmuir*, **26** (22), 16730–16736.

51 Huyal, I.O., Ozel, T., Tuncel, D., and Demir, H.V. (2008) Quantum efficiency enhancement in film by making nanoparticles of polyfluorene. *Opt. Express*, **16** (17), 13391–13397.

52 Park, E.-J., Erdem, T., Ibrahimova, V., Nizamoglu, S., Demir, H.V., and Tuncel, D. (2011) White-emitting conjugated polymer nanoparticles with cross-linked shell for mechanical stability and controllable photometric properties in color-conversion LED applications. *ACS Nano*, **5** (4), 2483–2492.

53 Huebner, C.F., Roeder, R.D., and Foulger, S.H. (2009) Nanoparticle electroluminescence: controlling emission color through Förster resonance energy transfer in hybrid particles. *Adv. Funct. Mater.*, **19** (22), 3604–3609.

54 Huebner, C.F., Carroll, J.B., Evanoff, D. D., Ying, Y., Stevenson, B.J., Lawrence, J. R., Houchins, J.M., Foguth, A.L., Sperry, J., and Foulger, S.H. (2008) Electroluminescent colloidal inks for flexographic roll-to-roll printing. *J. Mater. Chem.*, **18** (41), 4942–4948.

55 Chang, Y.-L., Palacios, R.E., Fan, F.-R.F., Bard, A.J., and Barbara, P.F. (2008) Electrogenerated chemiluminescence of single conjugated polymer nanoparticles. *J. Am. Chem. Soc.*, **130** (28), 8906–8907.

56 Palacios, R.E., Fan, F.-R.F., Grey, J.K., Suk, J., Bard, A.J., and Barbara, P.F. (2007) Charging and discharging of single conjugated-polymer nanoparticles. *Nat. Mater.*, **6** (9), 680–685.

57 Abbel, R., Wolffs, M., Bovee, R.A.A., van Dongen, J.L.J., Lou, X., Henze, O., Feast, W.J., Meijer, E.W., and Schenning, A.P.H. J. (2009) Side-chain degradation of ultrapure π-conjugated oligomers: implications for organic electronics. *Adv. Mater.*, **21** (5), 597–602.

58 List, E.J., Guentner, R., Scanducci de Freitas, P., and Scherf, U. (2002) The effect of keto defect sites on the emission properties of polyfluorene-type materials. *Adv. Mater.*, **14** (5), 374–378.

59 Grisorio, R., Suranna, G.P., Mastrorilli, P., and Nobile, C.F. (2007) Insight into the role of oxidation in the thermally induced green band in fluorene-based systems. *Adv. Funct. Mater.*, **17** (4), 538–548.

60 Pras, O., Chaussy, D., Stephan, O., Rharbi, Y., Piette, P., and Beneventi, D. (2010) Photoluminescence of 2,7-poly(9,9-dialkylfluorene-*co*-fluorenone) nanoparticles: effect of particle size and inert polymer addition. *Langmuir*, **26** (18), 14437–14442.

61 Sarrazin, P., Beneventi, D., Denneulin, A., Stephan, O., and Chaussy, D. (2010) Photoluminescent patterned papers resulting from printings of polymeric nanoparticles suspension. *Int. J. Polym. Sci.*, **2010**, 1–8.

62 Morteani, A.C., Sreearunothai, P., Herz, L.M., Friend, R.H., and Silva, C. (2004) Exciton regeneration at polymeric semiconductor heterojunctions. *Phys. Rev. Lett.*, **92** (24), 247402.

63 Morteani, A.C., Dhoot, A.S., Kim, J.-S., Silva, C., Greenham, N.C., Murphy, C., Moons, E., Ciná, S., Burroughes, J.H., and Friend, R.H. (2003) Barrier-free electron–hole capture in polymer blend heterojunction light-emitting diodes. *Adv. Mater.*, **15** (20), 1708–1712.

64 Arias, A.C., MacKenzie, J.D., Stevenson, R., Halls, J.J.M., Inbasekaran, M., Woo, E. P., Richards, D., and Friend, R.H. (2001) Photovoltaic performance and morphology of polyfluorene blends: a combined microscopic and photovoltaic investigation. *Macromolecules*, **34** (17), 6005–6013.

65 Snaith, H.J., Arias, A.C., Morteani, A.C., Silva, C., and Friend, R.H. (2002) Charge

generation kinetics and transport mechanisms in blended polyfluorene photovoltaic devices. *Nano Lett.*, **2** (12), 1353–1357.

66 Kietzke, T., Neher, D., Landfester, K., Montenegro, R., Guntner, R., and Scherf, U. (2003) Novel approaches to polymer blends based on polymer nanoparticles. *Nat. Mater.*, **2** (6), 408–412.

67 Kietzke, T., Neher, D., Kumke, M., Montenegro, R., Landfester, K., and Scherf, U. (2004) A nanoparticle approach to control the phase separation in polyfluorene photovoltaic devices. *Macromolecules*, **37** (13), 4882–4890.

68 Snaith, H.J. and Friend, R.H. (2004) Photovoltaic devices fabricated from an aqueous dispersion of polyfluorene nanoparticles using an electroplating method. *Synth. Met.*, **147** (1–3), 105–109.

69 Wu, C., Szymanski, C., Cain, Z., and McNeill, J. (2007) Conjugated polymer dots for multiphoton fluorescence imaging. *J. Am. Chem. Soc.*, **129** (43), 12904–12905.

70 Wu, C., Bull, B., Szymanski, C., Christensen, K., and McNeill, J. (2008) Multicolor conjugated polymer dots for biological fluorescence imaging. *ACS Nano*, **2** (11), 2415–2423.

71 Yu, J., Wu, C., Sahu, S.P., Fernando, L.P., Szymanski, C., and McNeill, J. (2009) Nanoscale 3D tracking with conjugated polymer nanoparticles. *J. Am. Chem. Soc.*, **131** (51), 18410–18414.

72 Wu, C. and McNeill, J. (2008) Swelling-controlled polymer phase and fluorescence properties of polyfluorene nanoparticles. *Langmuir*, **24** (11), 5855–5861.

73 Cadby, A.J., Lane, P.A., Mellor, H., Martin, S.J., Grell, M., Giebeler, C., Bradley, D.D. C., Wohlgenannt, M., An, C., and Vardeny, Z.V. (2000) Film morphology and photophysics of polyfluorene. *Phys. Rev. B*, **62** (23), 15604–15609.

74 Zhu, L., Qin, J., and Yang, C. (2010) Synthesis, photophysical properties, and self-assembly behavior of amphiphilic polyfluorene: unique dual fluorescence and its application as a fluorescent probe for the mercury ion. *J. Phys. Chem. B*, **114** (46), 14884–14889.

75 Yao, J.H., Mya, K.Y., Shen, L., He, B.P., Li, L., Li, Z.H., Chen, Z.-K., Li, X., and Loh, K.P. (2008) Fluorescent nanoparticles comprising amphiphilic rod–coil graft copolymers. *Macromolecules*, **41** (4), 1438–1443.

76 Tu, G., Li, H., Forster, M., Heiderhoff, R., Balk, L.J., Sigel, R., and Scherf, U. (2007) Amphiphilic conjugated block copolymers: synthesis and solvent-selective photoluminescence quenching. *Small*, **3** (6), 1001–1006.

77 Thivierge, C., Loudet, A., and Burgess, K. (2011) Brilliant BODIPY–fluorene copolymers with dispersed absorption and emission maxima. *Macromolecules*, **44** (10), 4012–4015.

78 Scherf, U., Adamczyk, S., Gutacker, A., and Koenen, N. (2009) All-conjugated, rod–rod block copolymers – generation and self-assembly properties. *Macromol. Rapid Commun.*, **30** (13), 1059–1065.

79 Tung, Y., Wu, W., and Chen, W. (2006) Morphological transformation and photophysical properties of rod–coil poly [2,7-(9,9-dihexylfluorene)]-*block*-poly (acrylic acid) in solution. *Macromol. Rapid Commun.*, **27** (21), 1838–1844.

80 Lin, S.-T., Tung, Y.-C., and Chen, W.-C. (2008) Synthesis, structures and multifunctional sensory properties of poly [2,7-(9,9-dihexylfluorene)]-*block*-poly[2-(dimethylamino)ethyl methacrylate] rod–coil diblock copolymers. *J. Mater. Chem.*, **18** (33), 3985–3992.

81 Yao, J.H., Mya, K.Y., Li, X., Parameswaran, M., Xu, Q.-H., Loh, K.P., and Chen, Z.-K. (2007) Light scattering and luminescence studies on self-aggregation behavior of amphiphilic copolymer micelles. *J. Phys. Chem. B*, **112** (3), 749–755.

82 Zhang, Z.-J., Qiang, L.-L., Liu, B., Xiao, X.-Q., Wei, W., Peng, B., and Huang, W. (2006) Synthesis and characterization of a novel water-soluble block copolymer with a rod–coil structure. *Mater. Lett.*, **60** (5), 679–684.

83 Wu, C., Peng, H., Jiang, Y., and McNeill, J. (2006) Energy transfer mediated fluorescence from blended conjugated polymer nanoparticles. *J. Phys. Chem. B*, **110** (29), 14148–14154.

84 Wu, C., Zheng, Y., Szymanski, C., and McNeill, J. (2008) Energy transfer in a nanoscale multichromophoric system: fluorescent dye-doped conjugated polymer nanoparticles. *J. Phys. Chem. C*, **112** (6), 1772–1781.

85 Jin, Y., Ye, F., Zeigler, M., Wu, C., and Chiu, D.T. (2011) Near-infrared fluorescent dye-doped semiconducting polymer dots. *ACS Nano*, **5** (2), 1468–1475.

86 Davis, C.M., Childress, E.S., and Harbron, E.J. (2011) Ensemble and single-particle fluorescence photomodulation in diarylethene-doped conjugated polymer nanoparticles. *J. Phys. Chem. C*, **115** (39), 19065–19073.

87 Tian, Z., Wu, W., and Li, A.D.Q. (2009) Photoswitchable fluorescent nanoparticles: preparation, properties and applications. *ChemPhysChem*, **10** (15), 2577–2591.

88 Acker, T. and Acker, H. (2004) Cellular oxygen sensing need in CNS function: physiological and pathological implications. *J. Exp. Biol.*, **207** (18), 3171–3188.

89 Carmeliet, P., Dor, Y., Herbert, J.-M., Fukumura, D., Brusselmans, K., Dewerchin, M., Neeman, M., Bono, F., Abramovitch, R., Maxwell, P., Koch, C.J., Ratcliffe, P., Moons, L., Jain, R.K., Collen, D., and Keshet, E. (1998) Role of HIF-1alpha in hypoxia-mediated apoptosis, cell proliferation and tumour angiogenesis. *Nature*, **394** (6692), 485–490.

90 DeBerardinis, R.J., Lum, J.J., Hatzivassiliou, G., and Thompson, C.B. (2008) The biology of cancer: metabolic reprogramming fuels cell growth and proliferation. *Cell Metab.*, **7** (1), 11–20.

91 Wang, J., Xu, X., Zhao, Y., Zheng, C., and Li, L. (2011) Exploring the application of conjugated polymer nanoparticles in chemical sensing: detection of free radicals by a synergy between fluorescent nanoparticles of two conjugated polymers. *J. Mater. Chem.*, **21** (46), 18696–18703.

92 Pecher, J., Huber, J., Winterhalder, M., Zumbusch, A., and Mecking, S. (2010) Tailor-made conjugated polymer nanoparticles for multicolor and multiphoton cell imaging. *Biomacromolecules*, **11** (10), 2776–2780.

93 Wang, R., Zhang, C., Wang, W., and Liu, T. (2010) Preparation, morphology, and biolabeling of fluorescent nanoparticles based on conjugated polymers by emulsion polymerization. *J. Polym. Sci. Part A: Polym. Chem.*, **48** (21), 4867–4874.

94 Kim, S., Lim, C.-K., Na, J., Lee, Y.-D., Kim, K., Choi, K., Leary, J.F., and Kwon, I.C. (2010) Conjugated polymer nanoparticles for biomedical *in vivo* imaging. *Chem. Commun.*, **46** (10), 1617–1619.

95 İbrahimova, V., Ekiz, S., Gezici, Ö., and Tuncel, D. (2011) Facile synthesis of cross-linked patchy fluorescent conjugated polymer nanoparticles by click reactions. *Polym. Chem.*, **2** (12), 2818–2824.

96 Hashim, Z., Howes, P., and Green, M. (2011) Luminescent quantum-dot-sized conjugated polymer nanoparticles – nanoparticle formation in a miniemulsion system. *J. Mater. Chem.*, **21** (6), 1797–1803.

97 Caliceti, P. and Veronese, F.M. (2003) Pharmacokinetic and biodistribution properties of poly(ethylene glycol)–protein conjugates. *Adv. Drug Deliv. Rev.*, **55** (10), 1261–1277.

98 Karakoti, A.S., Das, S., Thevuthasan, S., and Seal, S. (2011) PEGylated inorganic nanoparticles. *Angew. Chem., Int. Ed.*, **50** (9), 1980–1994.

99 Kandel, P.K., Fernando, L.P., Ackroyd, P. C., and Christensen, K.A. (2011) Incorporating functionalized polyethylene glycol lipids into reprecipitated conjugated polymer nanoparticles for bioconjugation and targeted labeling of cells. *Nanoscale*, **3** (3), 1037–1045.

100 Howes, P., Green, M., Levitt, J., Suhling, K., and Hughes, M. (2010) Phospholipid encapsulated semiconducting polymer nanoparticles: their use in cell imaging and protein attachment. *J. Am. Chem. Soc.*, **132** (11), 3989–3996.

101 Howes, P., Green, M., Bowers, A., Parker, D., Varma, G., Kallumadil, M., Hughes, M., Warley, A., Brain, A., and Botnar, R. (2010) Magnetic conjugated polymer nanoparticles as bimodal imaging agents. *J. Am. Chem. Soc.*, **132** (28), 9833–9842.

102 Lee, C.-S., Chang, H.H., Jung, J., Lee, N. A., Song, N.W., and Chung, B.H. (2012) A novel fluorescent nanoparticle composed of fluorene copolymer core and silica shell with enhanced photostability. *Colloids Surf. B*, **91** (0), 219–225.

103 Li, K., Pan, J., Feng, S., Wu, A.W., Pu, K., Liu, Y., and Liu, B. (2009) Generic strategy of preparing fluorescent conjugated-polymer-loaded poly(DL-lactide-*co*-glycolide) nanoparticles for targeted cell imaging. *Adv. Funct. Mater.*, **19** (22), 3535–3542.

104 Li, K., Zhan, R., Feng, S.-S., and Liu, B. (2011) Conjugated polymer loaded nanospheres with surface functionalization for simultaneous discrimination of different live cancer cells under single wavelength excitation. *Anal. Chem.*, **83** (6), 2125–2132.

105 Wu, C., Jin, Y., Schneider, T., Burnham, D.R., Smith, P.B., and Chiu, D.T. (2010) Ultrabright and bioorthogonal labeling of cellular targets using semiconducting polymer dots and click chemistry. *Angew. Chem., Int. Ed.*, **49** (49), 9436–9440.

106 Wu, C., Schneider, T., Zeigler, M., Yu, J., Schiro, P.G., Burnham, D.R., McNeill, J.D., and Chiu, D.T. (2010) Bioconjugation of ultrabright semiconducting polymer dots for specific cellular targeting. *J. Am. Chem. Soc.*, **132** (43), 15410–15417.

107 Wu, C., Hansen, S.J., Hou, Q., Yu, J., Zeigler, M., Jin, Y., Burnham, D.R., McNeill, J.D., Olson, J.M., and Chiu, D.T. (2011) Design of highly emissive polymer dot bioconjugates for *in vivo* tumor targeting. *Angew. Chem., Int. Ed.*, **50** (15), 3430–3434.

108 Chan, Y.-H., Jin, Y., Wu, C., and Chiu, D. T. (2011) Copper(II) and iron(II) ion sensing with semiconducting polymer dots. *Chem. Commun.*, **47** (10), 2820–2822.

109 Abbel, R., van der Weegen, R., Meijer, E. W., and Schenning, A.P.H.J. (2009) Multicolour self-assembled particles of fluorene-based bolaamphiphiles. *Chem. Commun.*, **13**, 1697–1699.

110 Vijayakumar, C., Sugiyasu, K., and Takeuchi, M. (2011) Oligofluorene-based electrophoretic nanoparticles in aqueous medium as a donor scaffold for fluorescence resonance energy transfer and white-light emission. *Chem. Sci.*, **2** (2), 291–294.

111 Tseng, K.-P., Fang, F.-C., Shyue, J.-J., Wong, K.-T., Raffy, G., Del Guerzo, A., and Bassani, D.M. (2011) Spontaneous generation of highly emissive RGB organic nanospheres. *Angew. Chem., Int. Ed.*, **50** (31), 7032–7036.

112 Koizumi, Y., Seki, S., Tsukuda, S., Sakamoto, S., and Tagawa, S. (2006) Self-condensed nanoparticles of oligofluorenes with water-soluble side chains. *J. Am. Chem. Soc.*, **128** (28), 9036–9037.

113 Zhu, L., Yang, C., and Qin, J. (2008) An aggregation-induced blue shift of emission and the self-assembly of nanoparticles from a novel amphiphilic oligofluorene. *Chem. Commun.*, (47), 6303–6305.

114 Petkau, K., Kaeser, A., Fischer, I., Brunsveld, L., and Schenning, A.P.H.J. (2011) Pre- and postfunctionalized self-assembled π-conjugated fluorescent organic nanoparticles for dual targeting. *J. Am. Chem. Soc.*, **133** (42), 17063–17071.

115 Suk, J., Cheng, J.-Z., Wong, K.-T., and Bard, A.J. (2011) Synthesis, electrochemistry, and electrogenerated chemiluminescence of azide-BTA, a D–A–π–A–D species with benzothiadiazole and *N,N*-diphenylaniline, and its nanoparticles. *J. Phys. Chem. C*, **115** (30), 14960–14968.

116 Schenning, A.P.H.J. and Meijer, E.W. (2005) Supramolecular electronics; nanowires from self-assembled π-conjugated systems. *Chem. Commun.*, (26), 3245–3258.